Report

Cell Reports

ABCB5 Identifies Immunoregulatory Dermal Cells

Graphical Abstract

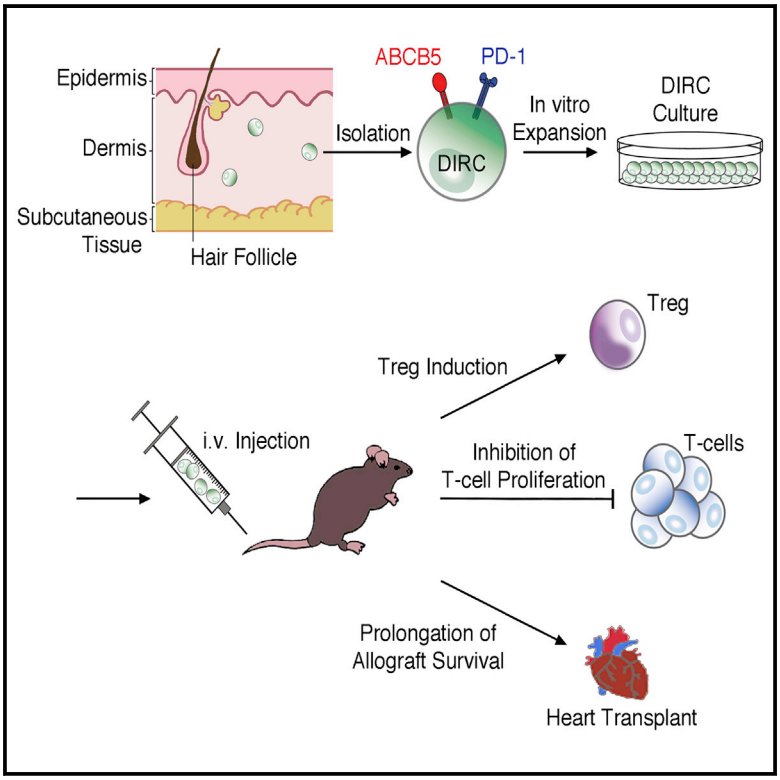

Highlights

- Mammalian skin contains dermal immunoregulatory cells (DIRCs)
- ABCB5 surface expression constitutes a molecular marker for the isolation of DIRCs
- DIRCs suppress alloimmunity and prolong cardiac allograft survival
- Efficient DIRC-mediated immunosuppression requires PD-1-mediated Treg induction

Authors

Tobias Schatton, Jun Yang, Sonja Kleffel, ..., Thomas S. Kupper, Natasha Y. Frank, Markus H. Frank

Correspondence

markus.frank@childrens.harvard.edu

In Brief

Schatton et al. identify ABCB5 as a marker of dermal cells in mammalian skin that possess immunoregulatory functions, through engagement of the immune checkpoint molecule PD-1. ABCB5-positive cells, when administered to recipients of heart transplants in preclinical models, prolong graft survival, suggesting promising roles of this cell subset in cellular immunotherapy.

Schatton et al., 2015, Cell Reports *12*, 1564–1574
September 8, 2015
http://dx.doi.org/10.1016/j.celrep.2015.08.010

OPEN ACCESS
CellPress

Cell Reports
Report

ABCB5 Identifies Immunoregulatory Dermal Cells

Tobias Schatton,[1,2] Jun Yang,[2,3] Sonja Kleffel,[1] Mayuko Uehara,[2] Steven R. Barthel,[1] Christoph Schlapbach,[1,4] Qian Zhan,[5] Stephen Dudeney,[1] Hansgeorg Mueller,[1] Nayoung Lee,[1] Juliane C. de Vries,[6] Barbara Meier,[6] Seppe Vander Beken,[6] Mark A. Kluth,[7] Christoph Ganss,[7] Arlene H. Sharpe,[5,8,9] Ana Maria Waaga-Gasser,[10] Mohamed H. Sayegh,[2] Reza Abdi,[2] Karin Scharffetter-Kochanek,[6] George F. Murphy,[5] Thomas S. Kupper,[1] Natasha Y. Frank,[2,11,12] and Markus H. Frank[1,2,13,*]

[1]Department of Dermatology, Brigham and Women's Hospital, Boston, MA 02115, USA
[2]Transplantation Research Center, Boston Children's Hospital and Brigham and Women's Hospital, Boston, MA 02115, USA
[3]Institute of Organ Transplantation, Huazhong University of Science and Technology, Wuhan 430074, China
[4]Department of Dermatology, University of Bern, Bern 3012, Switzerland
[5]Department of Pathology, Brigham and Women's Hospital, Boston, MA 02115, USA
[6]Department of Dermatology and Allergic Diseases, University of Ulm, Ulm 89077, Germany
[7]Rheacell GmbH & Co. KG, Heidelberg 69120, Germany
[8]Department of Microbiology and Immunobiology, Harvard Medical School, Boston, MA 02115, USA
[9]Evergrande Center for Immunologic Diseases, Brigham and Women's Hospital, Boston, MA 02115, USA
[10]Department of Surgery, University of Würzburg Medical School, Würzburg 97080, Germany
[11]Department of Medicine, Boston VA Healthcare System, West Roxbury, MA 02132, USA
[12]Division of Genetics, Brigham and Women's Hospital, Boston, MA 02115, USA
[13]School of Medical Sciences, Edith Cowan University, Joondalup, WA 6027, Australia
*Correspondence: markus.frank@childrens.harvard.edu
http://dx.doi.org/10.1016/j.celrep.2015.08.010

SUMMARY

Cell-based strategies represent a new frontier in the treatment of immune-mediated disorders. However, the paucity of markers for isolation of molecularly defined immunomodulatory cell populations poses a barrier to this field. Here, we show that ATP-binding cassette member B5 (ABCB5) identifies dermal immunoregulatory cells (DIRCs) capable of exerting therapeutic immunoregulatory functions through engagement of programmed cell death 1 (PD-1). Purified Abcb5$^+$ DIRCs suppressed T cell proliferation, evaded immune rejection, homed to recipient immune tissues, and induced Tregs in vivo. In fully major-histocompatibility-complex-mismatched cardiac allotransplantation models, allogeneic DIRCs significantly prolonged allograft survival. Blockade of DIRC-expressed PD-1 reversed the inhibitory effects of DIRCs on T cell activation, inhibited DIRC-dependent Treg induction, and attenuated DIRC-induced prolongation of cardiac allograft survival, indicating that DIRC immunoregulatory function is mediated, at least in part, through PD-1. Our results identify ABCB5$^+$ DIRCs as a distinct immunoregulatory cell population and suggest promising roles of this expandable cell subset in cellular immunotherapy.

INTRODUCTION

Skin contains large numbers of effector T cells, particularly in the dermis (Clark et al., 2006). Cutaneous immunity must therefore be tightly regulated to prevent inappropriate immune activation, while at the same time maintaining the ability to combat harmful pathogens. While this control is in part accomplished by resident tolerogenic immune cell populations, including Tregs (Dudda et al., 2008), we hypothesized that skin might additionally contain non-hematopoietic lineage cell populations with immunoregulatory functions, with potential similarity to immunoregulatory mesenchymal stem cells (MSCs) in other tissues (Uccelli et al., 2008). We reasoned that this possibility, if correct, would then provide for relatively easily accessible cell populations for use in cell-based immunomodulatory strategies. We further hypothesized that the stem cell marker (Ksander et al., 2014) ABCB5 might identify such cell populations in normal skin, given its original discovery as a molecular determinant of skin-associated tissue precursors (Frank et al., 2003; Schatton et al., 2008) and immunoregulatory cell subsets in skin-associated malignancy (Schatton et al., 2010).

RESULTS

Human Dermis Contains a Cell Population Marked by ABCB5

We first characterized ABCB5 expression in healthy human skin. Immunostaining revealed that ABCB5$^+$ cell subsets reside in the reticular dermis (Figure 1A) at frequencies ranging from 1.5% to 4.0% of dermal cells (2.5% ± 0.8%, mean ± SE, n = 3 donors, Figure 1B) and that this subpopulation is distinct from CD34$^+$ dermal dendritic cells, neighboring fibroblasts, or CD31$^+$ endothelial cells (Figure 1C). Flow cytometric analyses confirmed negativity of ABCB5$^+$ skin cells for CD34, a marker of dermal dendritic cells and hematopoietic stem cells, and CD31, a marker of endothelial lineage differentiation (Figure 1D). Furthermore, ABCB5$^+$ skin cells exhibited negativity

for the pan-hematopoietic lineage marker, CD45 (Figure 1D), documenting absence of overlap with skin-resident immune cell populations. While ABCB5$^+$ skin cells preferentially co-expressed the MSC markers CD29, CD44, CD49e, CD73, CD105, and CD166 on >90% of cells, respectively, only distinct subpopulations of cells with positivity for each MSC marker exhibited positivity for ABCB5 (Figure 1D), demonstrating that ABCB5 identifies a previously unrecognized and phenotypically unique dermal cell subset.

ABCB5$^+$ Skin Cells Preferentially Express the Immune Checkpoint Receptor PD-1

Given the preferential association of MSC marker-positive (Frank et al., 2005), ABCB5-expressing cell subsets in skin-associated malignancy (Schatton et al., 2008) with immune checkpoint molecules, including PD-1 (Schatton et al., 2010), we next characterized the PD-1 pathway repertoire of ABCB5$^+$ skin cells. Immunofluorescence double staining of human skin sections revealed preferential coexpression of ABCB5 with PD-1 and demonstrated that this subpopulation is cytologically distinct from CD45$^+$ skin-associated lymphocytes (Figure 1E). Flow cytometric analysis of single cell suspensions derived from human skin biopsies (n = 4 donors) further confirmed PD-1 expression by CD45$^-$ human skin cells at relative frequencies not significantly different from those observed in CD45$^+$ lymphocytic skin infiltrates (Figure 1F, 16.0% ± 3.6% versus 15.3% ± 3.7%, mean ± SE, not significant [NS]). ABCB5$^+$CD45$^-$ cells isolated from human skin also demonstrated expression of PD-1 mRNA, as determined by RT-PCR amplification of the full coding sequence (CDS) of the human PD-1 (PDCD1) gene (Figure 1G). Moreover, quantitative real-time PCR revealed preferential expression of PD-1 mRNA by purified ABCB5$^+$ versus ABCB5$^-$ skin cells (Figure 1H and 1.2 ± 0.2-fold versus 0.5 ± 0.1-fold expression compared with detection in peripheral blood mononuclear cells (PBMCs), mean ± SE, $p < 0.05$). Preferential PD-1 expression at the protein level by ABCB5$^+$ compared to ABCB5$^-$ skin cells was shown by triple-color flow cytometry of single cell suspensions derived from human skin (Figure 1I, 90.9% ± 4.6% versus 9.1% ± 4.6% of CD45$^-$ skin cells, mean ± SE, $p < 0.001$). ABCB5$^+$ subpopulations did not express the costimulatory ligands PD-L1, PD-L2, B7.1 (CD80), or B7.2 (CD86) at significant levels (results not illustrated). Together, these findings demonstrate preferential expression of the immunologic checkpoint receptor, PD-1, by human ABCB5$^+$ skin cells.

Murine Skin Contains Abcb5$^+$ Dermal Cells that Preferentially Express PD-1

In order to explore the immunoregulatory roles of this dermal cell population in murine syngeneic and allogeneic in vivo models, we characterized its presence and molecular phenotype also in murine skin. Immunofluorescence staining revealed rare Abcb5$^+$ cells residing in the dermis but not in the epidermis or hair follicle (Figure 2A), consistent with findings in human skin (Figure 1A). Flow cytometry of single cell suspensions derived from murine (BALB/c) skin also revealed preferential PD-1 expression by Abcb5$^+$ compared to Abcb5$^-$ skin cells (Figure 2B, 46.8% ± 7.6% versus 4.0% ± 0.7% of CD45$^-$ skin cells, mean ± SE, $p < 0.001$), consistent with findings in human skin (Figure 1I). Moreover, immunofluorescence double staining of murine skin sections further confirmed preferential coexpression of Abcb5 with PD-1 and showed that murine skin contains PD-1$^+$CD45$^-$ cells, in addition to PD-1$^+$CD45$^+$ lymphocytes (Figure 2C). Additionally, in a side-by-side human/mouse immunoenzymatic staining experiment across the anastomosis of human skin to Rag2$^{-/-}$ mouse xenografts, using an anti-ABCB5 monoclonal antibody (mAb) directed against a species-conserved extracellular epitope of the molecule (Frank et al., 2003), we confirmed the exclusive localization of human ABCB5$^+$ and mouse Abcb5$^+$ cell populations to the dermis (Figure 2D), with human ABCB5$^+$ dermal cells in anastomosing skin readily distinguishable from murine Abcb5$^+$ cell subsets by co-staining for human-specific major histocompatibility complex (MHC) class I (Figure 2E). The incidentally observed relative increase of ABCB5$^+$ cell frequency at the site of anastomosis (Figure 2D) suggests activation of this cell population during the wound healing response. Next, we developed a protocol for isolating, cloning, propagating, and expanding murine Abcb5$^+$ dermal cells in vitro, under defined medium conditions already employed previously for the culture of human ABCB5$^+$ progenitor cells (Frank et al., 2003). Flow cytometric analysis of clonally derived murine dermal cell cultures revealed Abcb5 expression by the majority of cells in early passages (Figure 2F). Further characterization with respect to MSC antigens (Uccelli et al., 2008) demonstrated high expression of CD29, CD44, CD49e, CD73, CD105, and CD166 and absence of significant levels of CD31, CD34, or CD45 expression (Figure 2F), consistent with findings in human ABCB5$^+$ dermal cells (Figure 1D). Additionally, like human ABCB5$^+$ dermal cells, murine Abcb5$^+$ cells showed marked positivity for the co-inhibitory receptor, PD-1, in early passages, as determined by flow cytometry (Figure 2G) and RT-PCR amplification of the full CDS of the molecule (Figure 2H). While murine dermal cells exhibited increasingly lower PD-1 expression during ex vivo culture, possibly due to absent functional requirement or physiological stimuli, they nevertheless maintained a PD-1$^+$ cell population (cell frequency 6.8% ± 0.8%, mean ± SE) throughout later passages (Figure 2I).

Abcb5 Marks Dermal Immunoregulatory Cells that Suppress Alloantigen- and Mitogen-Dependent Immunity

To investigate the immunomodulatory capacity of Abcb5$^+$ dermal immunoregulatory cells (DIRCs), we grafted 3×10^6 syngeneic C57BL/6-derived DIRCs or fully MHC-mismatched BALB/c-derived DIRCs intravenously (i.v.) to C57BL/6 recipient mice (Figure 3A). Seven days post injection, we harvested the spleens of recipient mice and performed standard one-way mixed lymphocyte reactions (MLRs) using irradiated naive BALB/c or C3H/HeJ splenocytes as stimulators, as well as mitogen-stimulated proliferation assays. In vivo administration of either syngeneic or allogeneic DIRCs to C57BL/6 recipients significantly inhibited alloantigen-dependent T cell proliferation in the respective MLRs in a dose-dependent manner from 37%–91%, when compared to untreated control splenocytes (Figure 3B, $p < 0.001$ at 1:1 stimulator to responder ratios,

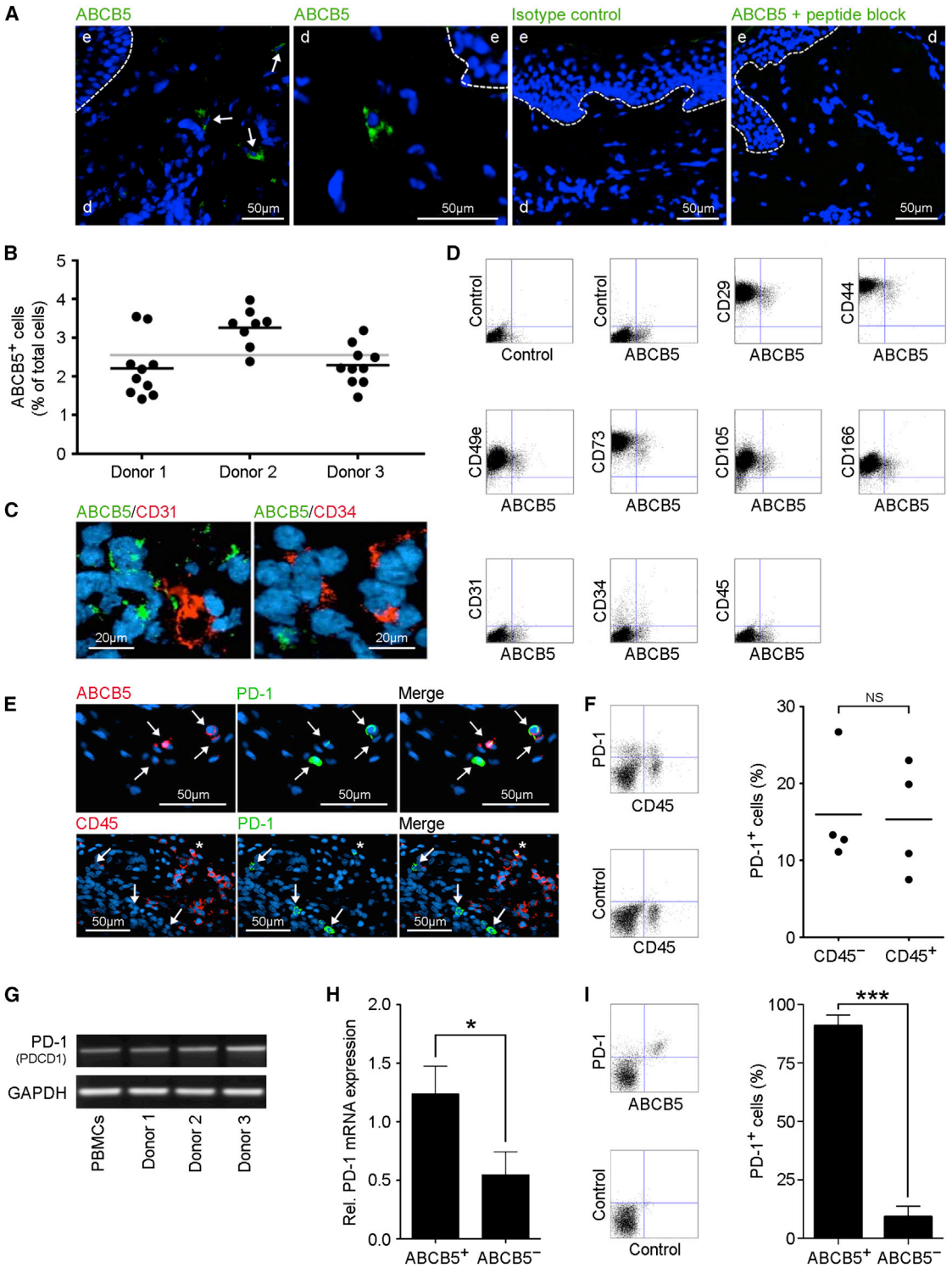

Figure 1. Characterization of ABCB5⁺ Dermal Cell Subpopulations in Human Skin

(A) Representative immunofluorescence staining of ABCB5 protein expression (green) in human skin (left and center left, arrows identify ABCB5⁺ cells). The specificity of the anti-ABCB5 staining was assessed using an isotype-matched control antibody (center-right) and by a peptide competition assay (right, pre-incubation of the ABCB5 antibody with a peptide containing the amino acid sequence of the antibody binding epitope (Frank et al., 2003; Ksander et al., 2014)). Nuclei are counterstained with DAPI (blue). d, dermis; e, epidermis.

(legend continued on next page)

respectively). Moreover, in vivo grafting of either recipient-type or fully MHC-mismatched DIRCs significantly inhibited T cell proliferation in response to mitogens ($p < 0.01$, respectively) (Figure 3C). These findings showed that Abcb5$^+$ DIRCs possess the capacity to modulate primary immune responses in vivo. Systematic characterization of the in vivo trafficking pattern of i.v. grafted Abcb5$^+$ DIRCs, using DiO fluorescent dye-labeled DIRC tracing by fluorescent microscopy of dissected tissues, hereby revealed that BALB/c-derived, fully MHC-mismatched DIRCs can withstand acute immune rejection, with DIRC presence 7 days post grafting to C57BL/6 recipients detected in every recipient tissue examined (range of engraftment frequencies: 2.7 ± 0.8 (muscle) to 37.0 ± 6.3 (thymus) DiO$^+$ DIRCs per 1,000 nucleated tissue cells, mean ± SE, n = 3 mice) (Figure S1).

Intravenous Administration of DIRCs Prolongs Cardiac Allograft Survival

We next examined the in vivo immunomodulatory effects of DIRCs on alloimmune responses using a stringent murine heterotopic cardiac allotransplantion model (Figure 3A). In a fully MHC-mismatched strain combination, treatment of C57BL/6 recipients of BALB/c cardiac allografts with donor-type DIRCs 7 days before cardiac transplantation (3×10^6 cells i.v., n = 8) resulted in significant prolongation of allograft survival compared to donor-type splenocyte-treated (n = 4, not illustrated) or untreated control (n = 4) recipients (Figure 3D, median graft survival time [MST]: 19 versus 10 versus 7.5 days, $p < 0.001$, respectively), demonstrating in vivo efficacy of DIRCs to delay graft rejection. Furthermore, third-party, BALB/c strain DIRCs also markedly prolonged cardiac allograft survival in C57BL/6 recipients of C3H/HeJ hearts compared to controls (Figure 3D, MST: 24.5 versus 9 days, $p < 0.01$, n = 4, respectively), whereas C57BL/6 recipients of BALB/c cardiac allografts treated with recipient-strain DIRCs showed only modest prolongation of cardiac allograft survival (Figure 3D, MST: 10.5 versus 7.5 days, $p < 0.05$, n = 4, respectively). Thus, prolonged DIRC-dependent enhancement of cardiac allograft survival requires DIRC-dependent allogeneic stimulation. To demonstrate that inhibition of graft rejection is specifically mediated by Abcb5$^+$ dermal cells, we compared the ability of purified Abcb5$^+$ versus corresponding Abcb5$^-$ dermal cells to prolong cardiac allograft survival. Administration of BALB/c-derived Abcb5$^+$ DIRCs significantly ($p < 0.001$) prolonged allograft survival, whereas Abcb5$^-$ dermal cells did not augment survival of BALB/c hearts grafted to C57BL/6 mice, compared to untreated controls (Figure 3E, MST: 18.5 (n = 6) versus 6 (n = 5) versus 7 days (n = 11), respectively). Characterization of the tissue distribution pattern of DiO-labeled BALB/c DIRCs in C57BL/6 recipients of BALB/c hearts 10 days post cardiac allotransplantation (day 17) revealed low to absent DIRC levels in most tissues examined (Figure S2). However, as many as 1.9% of nucleated cells were DiO$^+$ DIRCs in the skin and thymus of recipient mice (Figure S2). Together with the finding of frequent absence of DIRCs in transplanted hearts (Figure S2, 0.9 ± 0.7 DIRCs per 1,000 nucleated tissue cells), our finding of relatively high DIRC frequencies in the thymus, in addition to native skin, suggests that DIRCs exert their immunomodulatory effect predominantly systemically, potentially by tolerizing thymic immune cells to alloantigens (also referred to as central tolerance [Hogquist et al., 2005]), as opposed to locally, in the cardiac allograft, by interacting with graft-infiltrating lymphocytes. Characterization of DIRCs with respect to molecules important for homing to the thymus (CCR7, E-selectin ligands) and skin (CCR4, CCR10, E-selectin ligands) (Sackstein, 2005) revealed expression of all four homing determinants by the majority of Abcb5$^+$ dermal cells (Figure S3), consistent with the observed tropism of i.v. administered DIRCs to thymus and skin.

DIRCs Induce Regulatory T Cells

To examine whether allogeneic DIRCs exert their immunoregulatory functions via the induction of tolerogenic immune populations, we quantified splenic Treg frequencies in DIRC-treated versus untreated control mice. BALB/c DIRC administration (3×10^6 cells, i.v.) resulted in increased CD4$^+$CD25$^+$Foxp3$^+$ Treg numbers in C57BL/6 recipients compared to controls (Figure 3F and 4.6% ± 0.3% (n = 10) versus 3.1% ± 0.4% (n = 6) mean ± SE, $p < 0.01$, day 7 respectively). Consistent with these results and our findings of marked cardiac allograft prolongation in donor- and third-party strain DIRC-treated, but not recipient-type DIRC-treated, allograft recipients compared to controls (Figure 3D), we found decreased cellular necrosis (Figure S4A) and 3-fold increased frequencies of intracardiac CD4$^+$Foxp3$^+$ Treg infiltrates in donor- and third-party strain DIRC-treated versus untreated animals (Figures 3G and S4B, n = 3 mice/group, $p < 0.0001$, respectively). Recipient-type DIRC administration, on the other hand, did not result in significant differences in intracardiac Treg numbers compared to cardiac allografts of untreated controls (Figure 3G, n = 3 mice, respectively).

(B) Quantification of ABCB5$^+$ cell frequency in human skin determined by immunofluorescence staining, as above, and counting of n = 8–10 independent skin sections per donor (n = 3).

(C) Immunofluorescence double staining (right panels) of ABCB5 (green) with CD31 or CD34 (red). Nuclei are counterstained with DAPI (blue).

(D) Representative flow cytometry of ABCB5 expression in human skin and representative dual-color flow cytometric analyses examining co-expression of ABCB5 with the MSC antigens CD29, CD44, CD49e, CD73, CD105 or CD166, the endothelial lineage marker CD31, the stem cell marker CD34, or the hematopoietic lineage marker CD45.

(E) Representative immunofluorescence double staining of ABCB5 (red) and PD-1 (green) expression (top panels; arrows: ABCB5$^+$PD-1$^+$ cells) and of CD45 (red) and PD-1 (green) expression (bottom panels; arrows: PD-1$^+$CD45$^-$ cells; asterisk: PD-1$^+$CD45$^+$ cell) in human skin specimens, with nuclei counterstained in blue.

(F) Flow cytometry of PD-1 expression by CD45$^+$ versus CD45$^-$ cells present in single cell suspension derived from human skin biopsies (left panels: representative plots; right panel: mean percentages, n = 4 patients).

(G) PD-1 mRNA expression in human patient-derived DIRC short-term cultures (less than passages), as determined by RT-PCR amplification of the full PD-1 CDS. Human PBMCs were used as a positive control.

(H) PD-1 mRNA expression (mean ± SE) determined by real-time PCR in ABCB5$^+$ vs. ABCB5$^-$ human skin isolates negative for the pan lymphocyte marker CD45.

(I) Representative flow cytometry plots (left) and mean percentages ±SE (right) of PD-1 protein expression by ABCB5$^+$ vs. ABCB5$^-$ human skin cells.

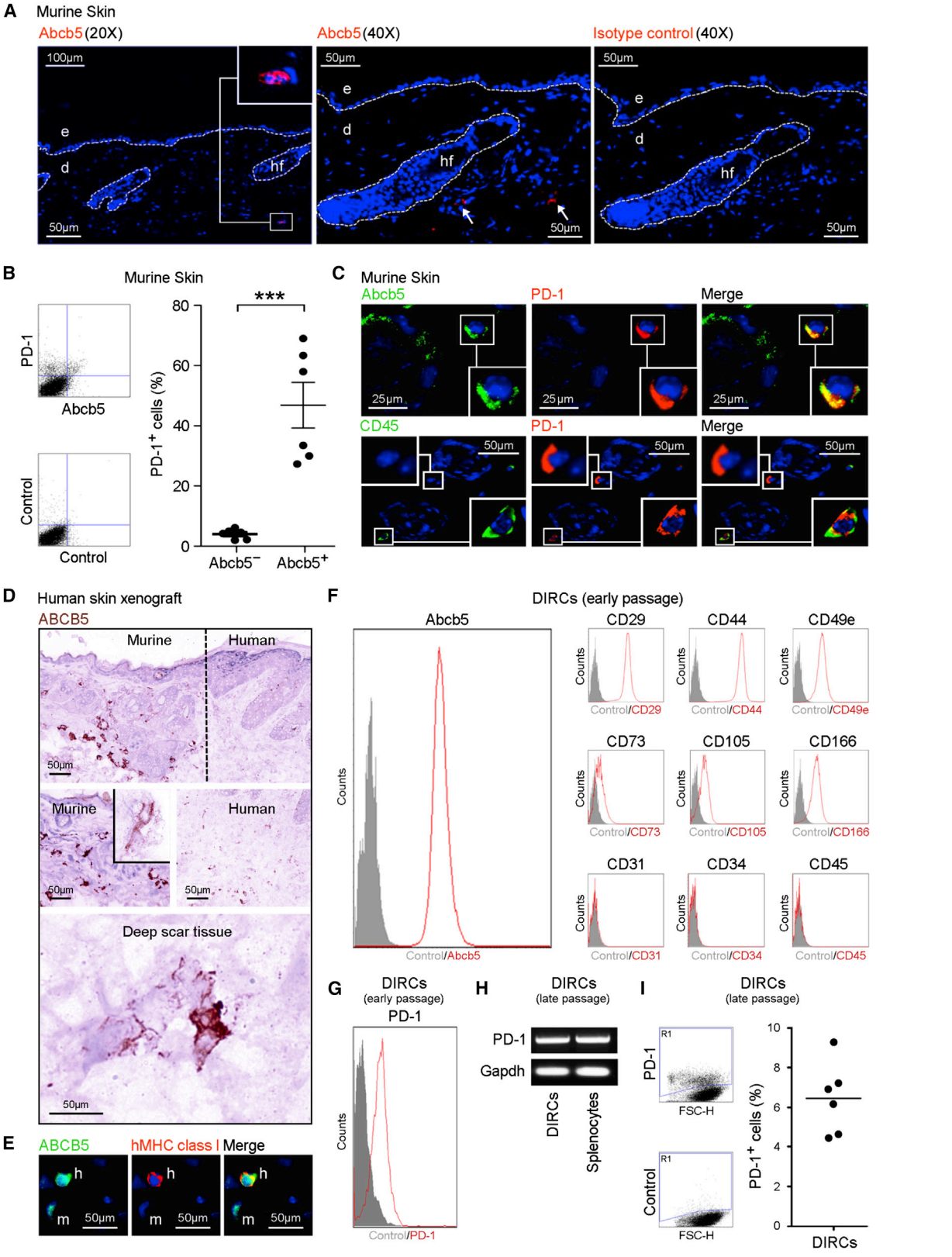

(legend on next page)

PD-1 Knockdown Reverses DIRC-Induced Regulatory T Cell Induction and Attenuates DIRC-Induced Prolongation of Cardiac Allograft Survival

PD-1-PD-L1 interactions represent a major immune checkpoint pathway (Francisco et al., 2010), with critical roles in Treg maintenance (Francisco et al., 2009; Wang et al., 2008). In order to investigate whether DIRC-expressed PD-1 is required for the immunomodulatory capacity of this cell subset, we generated stable PD-1 knockdown DIRC variants using PD-1 shRNA lentiviral particles. Significant PD-1 knockdown was shown both at the mRNA level by using RT-PCR and real-time PCR (Figure 4A, 60% knockdown) and at the protein level by using flow cytometric analysis (Figure 4A, >50% knockdown). To examine whether DIRC-expressed PD-1 has an inhibitory effect on T cell responses, we i.v. administered 3×10^6 control shRNA-transduced versus PD-1 knockdown BALB/c DIRCs to C57BL/6 recipients. Seven days post DIRC injection, we harvested the spleens of recipient animals and performed standard one-way MLRs as above (Figures 3B and 3C), using irradiated naive BALB/c or C3H/HeJ splenocytes as stimulators, or a mitogen-stimulated proliferation assay. Consistent with our findings using native DIRCs, in vivo administration of control shRNA-transduced DIRCs significantly inhibited alloantigen-dependent T cell proliferation in either MLR by >80% and >90% at 1:5 and 1:1 stimulator to responder ratios ($p < 0.01$), respectively (Figure 4B). We also found control DIRC transplantation to significantly ($p < 0.001$) inhibit ex vivo T cell proliferation in response to mitogens compared to controls (Figure 4C). Remarkably, DIRC-specific PD-1 knockdown significantly reversed the inhibitory effect of control DIRCs on T cell proliferation in both MLRs ($p < 0.01$, respectively) (Figure 4B and 3.9- and 5.2-fold [BALB/c MLR] versus 11.4- and 25.7-fold [C3H/HeJ MLR] increase in proliferation in PD-1 knockdown versus control DIRC treatment groups at 1:5 and 1:1 stimulator/responder ratios, respectively), as well as in response to mitogen stimulation (Figure 4C, $p < 0.05$). Additionally, while control shRNA-transduced BALB/c DIRC treatment, analogous to native BALB/c DIRCs (Figure 3F), significantly induced $CD4^+CD25^+Foxp3^+$ Tregs in C57BL/6 recipient spleens 7 days post i.v. DIRC administration compared to untreated controls (Figure 4D and 3.4% ± 0.3% (n = 7) versus 1.5% ± 0.2% (n = 9) mean ± SE, $p < 0.0001$, respectively), DIRC-specific PD-1 knockdown significantly reversed the Treg induction observed in control DIRC-treated mice to Treg levels not significantly different from those in untreated animals (Figure 4D and 1.7% ± 0.1% (n = 7) versus 1.5% ± 0.2% (n = 9) mean ± SE, NS, respectively). Furthermore, administration of PD-1-expressing, BALB/c-derived DIRCs to PD-L1($^{-/-}$) knockout (KO) C57BL/6 mice (Francisco et al., 2009) deficient in the predominant (Francisco et al., 2010) PD-1 ligand, PD-L1, did not significantly alter Treg numbers compared to untreated controls (Figure 4E), indicating a requirement for DIRC-PD-1:host-PD-L1 interactions for efficient DIRC-dependent Treg induction. Finally, administration of PD-1 knockdown DIRCs to C57BL/6 recipients of BALB/c hearts significantly attenuated DIRC-induced prolongation of cardiac allograft survival compared to control shRNA-transduced DIRCs (Figure 4F, MST: 10 versus 14 days, $p < 0.05$, n = 11, respectively), the latter of which exhibited allograft survival-prolonging effects not significantly different ($p > 0.05$) from wild-type DIRCs (Figure 3D). Together, these results identified a critical in vivo role of DIRC-expressed PD-1 in Treg induction and prolongation of cardiac allograft survival and established DIRC-expressed PD-1 as a previously unrecognized immunoregulatory mechanism.

DISCUSSION

Our study has several important implications. First, identification of molecularly defined DIRCs has the potential to decisively advance the field of cell-based immunotherapy, because, thus far, no molecular marker has been available for the prospective isolation of comparably potent non-hematopoietic immunoregulatory cell subsets with defined mechanism of action from any adult tissue. Bone marrow (BM)-derived MSCs display similar molecular profiles such as CD29, CD73, and CD105 expression with negativity for the hematopoietic lineage antigens, CD34 and CD45 (Uccelli et al., 2008), and have previously been found to suppress T cell proliferation to alloantigens and mitogens (Bartholomew et al., 2002), evade immunologic rejection (Devine et al., 2003), regulate Treg function (Casiraghi et al., 2008), and modulate alloimmune responses in preclinical animal models (Bartholomew et al., 2002; Casiraghi et al., 2008). As a result, they have been extensively employed in cell-based immunomodulatory treatment strategies (Uccelli et al., 2008). However, unlike ABCB5-purified DIRCs, BM-MSCs cannot be enriched as pure populations by a single molecular marker and have thus far failed to consistently prolong allograft survival in fully MHC-mismatched recipients (Bartholomew et al., 2002; Inoue et al., 2006; Nauta et al., 2006). This

Figure 2. Characterization of $Abcb5^+$ Dermal Cell Subpopulations in Murine Skin

(A) Representative immunofluorescence staining of Abcb5 protein expression (red) in murine skin (left and center). The specificity of the anti-Abcb5 staining was assessed using an isotype-matched control antibody (right). Arrows in center panel identify $Abcb5^+$ cells. d, dermis; e, epidermis; hf, hair follicle.

(B and C) (B) Representative flow cytometry plots (left) and mean percentages (right) of PD-1 protein expression by $Abcb5^+$ versus $Abcb5^-$ murine (BALB/c) skin cells and (C) representative immunofluorescence double staining of Abcb5 (green) and PD-1 (red) expression (top panels) and of CD45 (green) and PD-1 (red) expression (bottom panels) in murine skin specimens, with nuclei counterstained in blue. Insets, high magnification.

(D) Immunohistochemical (IHC) analysis of ABCB5 expression across the anastomosis of a human skin to $Rag2^{-/-}$ mouse xenograft using an anti-ABCB5 mAb that recognizes both human ABCB5 and murine Abcb5. Isotype-matched negative controls established dermal cell binding of ABCB5 mAb as specific.

(E) Representative IHC images depicting co-expression of ABCB5 with human MHC class I in human skin xenografts, as above. h, human $ABCB5^+$hMHC class I^+ cell; m, murine $Abcb5^+$hMHC class I^- cell.

(F and G) (F) Representative flow cytometry of surface Abcb5, CD29, CD44, CD49e, CD73, CD105, CD166, CD31, CD34, and CD45 and of (G) PD-1 expression by early passage murine DIRC cultures.

(H) PD-1 mRNA expression by murine DIRCs as determined by RT-PCR amplification of the full murine PD-1 CDS and

(I) Representative flow cytometry plots (left) and mean percentages (right) of PD-1 protein expression by late passage murine DIRC cultures.

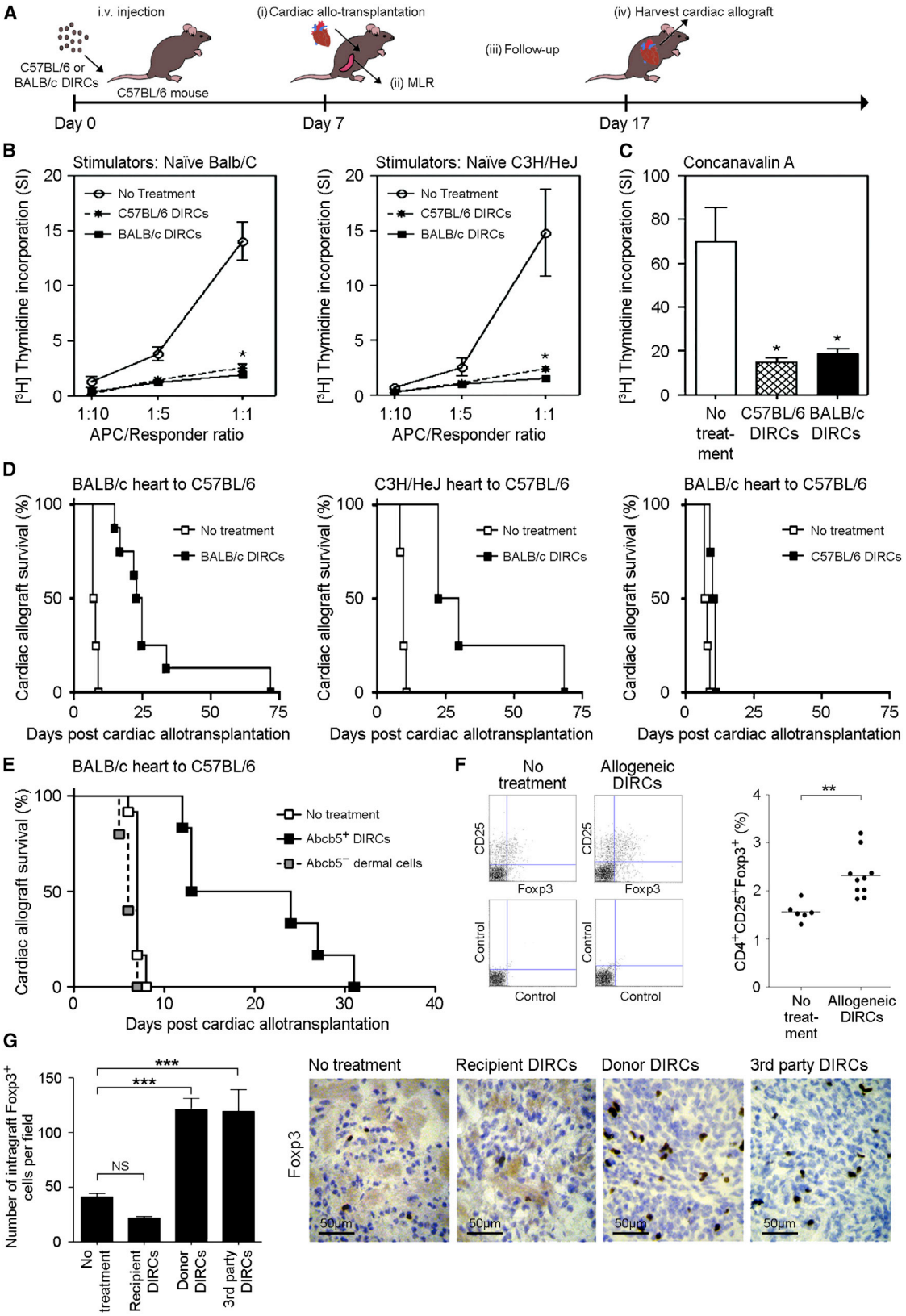

(legend on next page)

indicates that immunoregulatory ABCB5$^+$ DIRCs that also express the immune checkpoint regulator PD-1 might represent more effective in vivo modulators of allograft rejection. In our study, i.v. administered DIRCs contained across the various experiments at least >200,000 Abcb5$^+$PD-1$^+$ cells, a dose with consistent and reproducible immunomodulatory effects. Whether lower doses of DIRCs might also be effective, or whether higher doses or alternative dosing intervals might further enhance the herein documented immunomodulatory effects, deserves further investigation. Our results show that the immunoregulatory function of ABCB5$^+$ DIRCs is, at least in part, mediated through co-expressed PD-1, because PD-1 knockdown significantly attenuated DIRC-induced prolongation of cardiac allograft survival. However, since PD-1 knockdown did not fully reverse immunosuppressive DIRC function, it is possible that additional immunoregulatory mechanisms might be operative in DIRCs that are yet to be elucidated. The potential promise of molecularly purified DIRCs for use in cell-based immunotherapeutic strategies is underscored by the additional advantage of easy accessibility of skin as a tissue source of cell isolation.

Second, our work establishes PD-1 expression by normal tissue-specific non-immune cells and shows that DIRC-expressed PD-1 functions as a previously unrecognized immunoregulatory mechanism, similar to our recent demonstration that ABCB5$^+$ skin-associated malignant cells express PD-1 and preferentially activate Tregs (Schatton et al., 2010). The herein identified role of DIRC-expressed PD-1 in Treg induction resembles the established role of T cellular PD-1 in Treg induction via PD-1:PD-L1 signaling interactions (Francisco et al., 2009; Wang et al., 2008). Because Tregs represent dominant mediators of immune homeostasis (Hogquist et al., 2005), including in the skin (Dudda et al., 2008), our discovery of functional PD-1 expression by DIRCs supports the existence of a *dermal* mechanism, in addition to a previously demonstrated *epidermal*, Langerhans cell-mediated mechanism (Seneschal et al., 2012), of Treg maintenance in mammalian skin. This finding is of current clinical relevance also to human cancer, where PD-1 has evolved as a highly promising target for tumor immunotherapy, with recently completed clinical trials demonstrating objective response rates markedly exceeding those achieved with alternative immunotherapeutic regimens in patients with advanced disease (Postow et al., 2015). However, adverse clinical effects of PD-1 antibody treatment include the occurrence of autoimmune skin conditions, such as vitiligo (Postow et al., 2015). In light of our current discovery of functional PD-1 expression by immunoregulatory DIRCs, such autoimmune events could potentially be explained as a result of off-target inhibition of PD-1 on DIRCs, leading to dysregulation of DIRC-mediated skin immune homeostasis.

Finally, whereas stem cell populations from the epidermis and hair follicle have been extensively studied and thoroughly defined at the molecular level (Fuchs, 2007), additional MSC phenotype-expressing cell types from the dermis are currently less well understood. Our result that ABCB5$^+$ DIRCs represents a dermal cell subset with MSC phenotype warrants examination whether these cells, like MSCs (Uccelli et al., 2008), might possess multipotent differentiation plasticity and could therefore be suitable for evaluation of uses in regenerative medicine, beyond immunomodulation.

In aggregate, our results identify molecularly defined DIRCs as a skin-associated immunoregulatory cell population with promise for cellular immunotherapy applications. Moreover, they provide initial evidence for a role of non-immune cell-expressed PD-1 in immunoregulation.

EXPERIMENTAL PROCEDURES

Cell Isolation and Culture Methods

Single cell suspensions from human and murine skin specimens were generated as described (Schatton et al., 2008) and ABCB5$^+$/Abcb5$^+$ DIRCs isolated by positive selection as described (Schatton et al., 2008). DIRC cultures were maintained under previously described culture conditions (Frank et al., 2003).

Flow Cytometry, Immunohistochemistry, and Immunofluorescence Staining

Analysis of cell-surface marker expression on single cell suspensions was carried out by flow cytometry as described (Schatton et al., 2008, 2010). E-selectin ligand staining was performed by incubation with recombinant mouse E-selectin Fc, as described (Liu et al., 2006). Immunohistochemical or immunofluorescence staining was performed as described (Schatton et al., 2008, 2010).

RT-PCR, Real-Time Quantitative PCR, and Generation of Stable PD-1 Knockdown DIRCs

Full-length human PD-1 (*PDCD1*) and murine PD-1 (*Pdcd1*) were amplified from human and murine DIRCs, respectively, following reverse transcription

Figure 3. Immunoregulatory Effects of Abcb5$^+$ DIRCs

(A) Diagram depicting the procedure for i.v. DIRC administration (day 0) and (i) abdominal heterotopic cardiac allotransplantation or (ii) spleen cell isolation for determination of ex vivo T cell proliferation by MLR (day 7). Cardiac allograft survival was (iii) monitored daily by palpation, with rejection defined as the complete cessation of detectable beating. For evaluation of lymphocytic infiltration and preservation of myocardium by immunohistochemistry, (iv) cardiac allograft were harvested on day 17.

(B) [^{3}H]thymidine incorporation (mean ± SE) of alloimmune stimulated C57BL/6 splenocytes plotted against increasing stimulator to responder ratios. Stimulators: naive irradiated BALB/c (left) or C3H/HeJ (right) splenocytes. Responders: untreated, C57BL/6 DIRC- or BALB/c DIRC-treated C57BL/6 recipient splenocytes.

(C) [^{3}H]thymidine uptake (mean ± SE) of mitogen-stimulated splenocytes in experimental groups as in (B).

(D and E) (D) Kaplan-Meier analysis of graft survival in BALB/c DIRC-treated C57BL/6 recipients of BALB/c (left) or C3H/HeJ donor hearts (center), and C57BL/6 DIRC-treated C57BL/6 recipients of BALB/c donor hearts (right), or of (E) Abcb5$^+$ DIRC- versus matched Abcb5$^-$ BALB/c-derived dermal cell-treated C57BL/6 recipients of BALB/c donor hearts.

(F) Representative flow cytometry plots (left) and mean percentages (right) of splenic CD4$^+$CD25$^+$Foxp3$^+$ Treg cells in untreated versus BALB/c DIRC-treated C57BL/6 recipient mice.

(G) Left panel: quantification of Foxp3$^+$ Treg cells in cardiac allografts of untreated, recipient-type-, donor-type-, or third-party strain DIRC-treated C57BL/6 recipients. Bars represent means ± SE of the total number of Foxp3-expressing cells per field of view. Triplicate images for n = 3 mice per group were analyzed. Right panels: a representative picture of Foxp3 immunohistochemical staining on intracardiac infiltrates for each experimental group is shown.

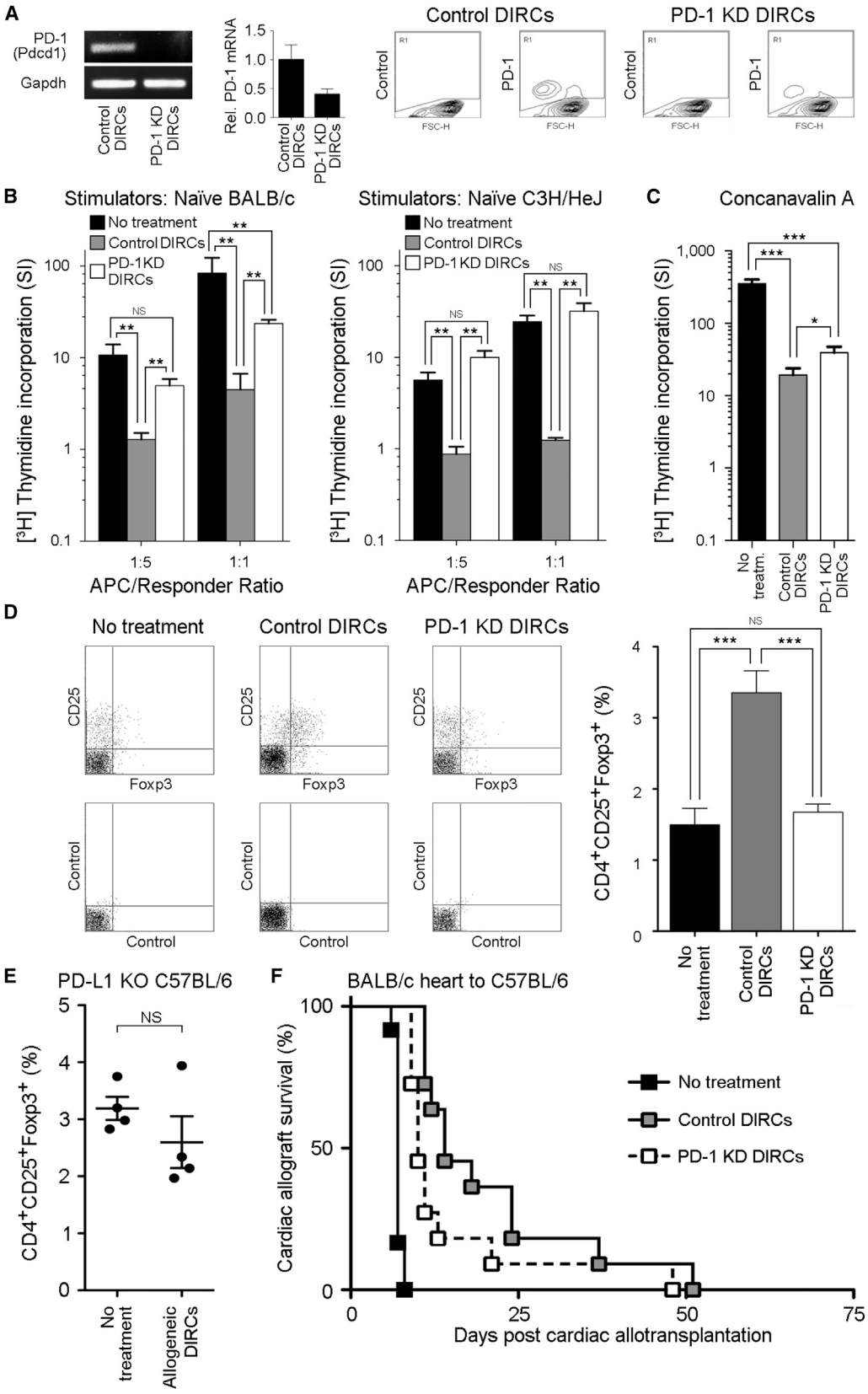

(legend on next page)

of total mRNA using *PDCD1*/*Pdcd1*-specific primer pairs. Relative *PDCD1*/*Pdcd1* transcript levels were determined by real-time quantitative RT-PCR and calculated using the $2^{(-\Delta\Delta Ct)}$ method as described previously (Frank et al., 2003; Schatton et al., 2008). Stable PD-1 knockdown DIRCs were generated using lentiviral transduction particles containing shRNAs against murine *Pdcd1*. PD-1 knockdown was confirmed by quantitative RT-PCR and by flow cytometry.

Mixed Lymphocyte Reaction, Heart Transplantation, In Vivo DIRC Tracking, and Human Skin Xenotransplantation

C57BL/6 ($H2^b$), BALB/c ($H2^d$), C3H/HeJ ($H2^k$), $Rag2^{-/-}$, and PD-L1($^{-/-}$) KO C57BL/6 mice (Francisco et al., 2009) were maintained and experiments performed under approved protocols in accordance with the Harvard Medical School Standing Committee on Animals and National Institutes of Animal Healthcare guidelines. To determine the effect of in vivo DIRC administration on Treg induction and lymphocyte activation, 3×10^6 DIRCs were injected i.v. to recipient mice, spleens were harvested 7 days post DIRC, and splenocytes were used for flow cytometric evaluation of Treg frequency or as responders in standard one-way MLRs as described (Izawa et al., 2010; Schatton et al., 2010). To determine the effect of i.v. injected DIRCs on murine cardiac allograft survival, abdominal heterotopic cardiac transplantation was performed by microsurgery, as described (Izawa et al., 2010), 7 days post DIRC administration. The in vivo distribution pattern of i.v.-administered DIRCs was assayed by DiO fluorescent cell labeling and subsequent fluorescence microscopy of recipient tissue, as described (Asahara et al., 1997). Human skin was obtained from discarded surgery specimens in accordance with the Partners Health Care Research Management Institutional Review Board and subsequently xenografted onto immunodeficient $Rag2^{-/-}$ mice as described (Juhasz et al., 1993).

Statistics

Statistical differences in allograft survival were assessed as described previously (Izawa et al., 2010) using Kaplan-Meier graphs and the log-rank test or, for comparison of median survival, the nonparametric Mann-Whitney test. Results of cell proliferation (MLRs), flow cytometry, and quantitative PCR assays were compared statistically using the unpaired Student's t test or the nonparametric Mann-Whitney test (comparison of two experimental groups) or one-way ANOVA followed by the Bonferroni correction (comparison of three or more experimental groups) (Izawa et al., 2010; Schatton et al., 2008, 2010). A two-sided p value <0.05 was considered statistically significant.

SUPPLEMENTAL INFORMATION

Supplemental Information includes Supplemental Experimental Procedures and four figures and can be found with this article online at http://dx.doi.org/10.1016/j.celrep.2015.08.010.

ACKNOWLEDGMENTS

This work was supported by NIH/NCI grants R01CA113796, R01CA158467, and R01CA138231 (to M.H.F.), the Department of Veterans Affairs VA Merit Review Awards VA BLR&D 1I01BX000516 and VA RR&D 1I01RX000989 (to N.Y.F.), by a grant RTG/CEMMA from the German Research Foundation (DFG) (to K.S.-K.), a Postdoctoral Fellowship Award from the American Heart Association, a Research Career Development Award from the Dermatology Foundation, and a Fund to Sustain Research Excellence from the Brigham Research Institute (to T.S.). T.S. is the recipient of an Innovative Research Grant from the Melanoma International Foundation and an NCI SPORE in Skin Cancer Developmental Project Grant. C.S. received salary support from the Swiss National Science Foundation, and C.S. and H.M. received salary support from the Fondation René Touraine. N.L. is the recipient of a Medical Student Grant from the American Skin Association.

M.H.F. is a co-inventor of the ABCB5-related US patent 6,846,883 (Gene encoding a multidrug resistance human P-glycoprotein homologue on chromosome 7p15-21 and uses thereof) assigned to Brigham and Women's Hospital, Boston, MA, and licensed to Ticeba GmbH (Heidelberg, Germany) and Rheacell GmbH & Co. KG (Heidelberg, Germany). M.H.F. serves as a scientific advisor to Ticeba GmbH and Rheacell GmbH & Co. KG. C.G. is CEO, and M.A.K. is CSO, of Rheacell GmbH & Co. KG. This work was supported in part by a grant from Rheacell GmbH & Co. KG.

Received: September 30, 2014
Revised: May 27, 2015
Accepted: August 4, 2015
Published: August 27, 2015

REFERENCES

Asahara, T., Murohara, T., Sullivan, A., Silver, M., van der Zee, R., Li, T., Witzenbichler, B., Schatteman, G., and Isner, J.M. (1997). Isolation of putative progenitor endothelial cells for angiogenesis. Science *275*, 964–967.

Bartholomew, A., Sturgeon, C., Siatskas, M., Ferrer, K., McIntosh, K., Patil, S., Hardy, W., Devine, S., Ucker, D., Deans, R., et al. (2002). Mesenchymal stem cells suppress lymphocyte proliferation in vitro and prolong skin graft survival in vivo. Exp. Hematol. *30*, 42–48.

Casiraghi, F., Azzollini, N., Cassis, P., Imberti, B., Morigi, M., Cugini, D., Cavinato, R.A., Todeschini, M., Solini, S., Sonzogni, A., et al. (2008). Pretransplant infusion of mesenchymal stem cells prolongs the survival of a semiallogeneic heart transplant through the generation of regulatory T cells. J. Immunol. *181*, 3933–3946.

Clark, R.A., Chong, B., Mirchandani, N., Brinster, N.K., Yamanaka, K., Dowgiert, R.K., and Kupper, T.S. (2006). The vast majority of CLA+ T cells are resident in normal skin. J. Immunol. *176*, 4431–4439.

Devine, S.M., Cobbs, C., Jennings, M., Bartholomew, A., and Hoffman, R. (2003). Mesenchymal stem cells distribute to a wide range of tissues following systemic infusion into nonhuman primates. Blood *101*, 2999–3001.

Dudda, J.C., Perdue, N., Bachtanian, E., and Campbell, D.J. (2008). Foxp3+ regulatory T cells maintain immune homeostasis in the skin. J. Exp. Med. *205*, 1559–1565.

Francisco, L.M., Salinas, V.H., Brown, K.E., Vanguri, V.K., Freeman, G.J., Kuchroo, V.K., and Sharpe, A.H. (2009). PD-L1 regulates the development, maintenance, and function of induced regulatory T cells. J. Exp. Med. *206*, 3015–3029.

Figure 4. Immunoregulatory Effects of PD-1 Expressed by DIRCs

(A) Stable PD-1 knockdown or scramble control BALB/c DIRCs were generated by using shRNA gene silencing. Confirmation of PD-1 knockdown was determined by RT-PCR (left), real-time PCR (center), or by flow cytometry (right).

(B) [^{3}H]-Thymidine incorporation (mean ± SE) of alloimmune stimulated C57BL/6 splenocytes at stimulator to responder ratios of 1:5 and 1:1, respectively. Stimulators: naive irradiated BALB/c (left) or C3H/HeJ (right) splenocytes. Responders: untreated, scrambled control- or PD-1 knockdown BALB/c DIRC-treated C57BL/6 recipient splenocytes.

(C) [^{3}H]thymidine uptake (mean ± SE) of mitogen-stimulated splenocytes in experimental groups as in (B).

(D and E) (D) Representative flow cytometry plots (left) and mean percentage ± SE (right) of splenic $CD4^+CD25^+Foxp3^+$ Treg frequencies in untreated, scrambled control- versus PD-1 knockdown BALB/c DIRC-treated C57BL/6 recipients, or in (E) untreated versus wild-type BALB/c DIRC-treated PD-L1($^{-/-}$) knockout (KO) C57BL/6 recipients.

(F) Kaplan-Meier analysis of graft survival in untreated, scrambled shRNA control- versus PD-1 knockdown BALB/c DIRC-treated C57BL/6 recipients of BALB/c donor hearts.

Francisco, L.M., Sage, P.T., and Sharpe, A.H. (2010). The PD-1 pathway in tolerance and autoimmunity. Immunol. Rev. *236*, 219–242.

Frank, N.Y., Pendse, S.S., Lapchak, P.H., Margaryan, A., Shlain, D., Doeing, C., Sayegh, M.H., and Frank, M.H. (2003). Regulation of progenitor cell fusion by ABCB5 P-glycoprotein, a novel human ATP-binding cassette transporter. J. Biol. Chem. *278*, 47156–47165.

Frank, N.Y., Margaryan, A., Huang, Y., Schatton, T., Waaga-Gasser, A.M., Gasser, M., Sayegh, M.H., Sadee, W., and Frank, M.H. (2005). ABCB5-mediated doxorubicin transport and chemoresistance in human malignant melanoma. Cancer Res. *65*, 4320–4333.

Fuchs, E. (2007). Scratching the surface of skin development. Nature *445*, 834–842.

Hogquist, K.A., Baldwin, T.A., and Jameson, S.C. (2005). Central tolerance: learning self-control in the thymus. Nat. Rev. Immunol. *5*, 772–782.

Inoue, S., Popp, F.C., Koehl, G.E., Piso, P., Schlitt, H.J., Geissler, E.K., and Dahlke, M.H. (2006). Immunomodulatory effects of mesenchymal stem cells in a rat organ transplant model. Transplantation *81*, 1589–1595.

Izawa, A., Schatton, T., Frank, N.Y., Ueno, T., Yamaura, K., Pendse, S.S., Margaryan, A., Grimm, M., Gasser, M., Waaga-Gasser, A.M., et al. (2010). A novel in vivo regulatory role of P-glycoprotein in alloimmunity. Biochem. Biophys. Res. Commun. *394*, 646–652.

Juhasz, I., Albelda, S.M., Elder, D.E., Murphy, G.F., Adachi, K., Herlyn, D., Valyi-Nagy, I.T., and Herlyn, M. (1993). Growth and invasion of human melanomas in human skin grafted to immunodeficient mice. Am. J. Pathol. *143*, 528–537.

Ksander, B.R., Kolovou, P.E., Wilson, B.J., Saab, K.R., Guo, Q., Ma, J., McGuire, S.P., Gregory, M.S., Vincent, W.J., Perez, V.L., et al. (2014). ABCB5 is a limbal stem cell gene required for corneal development and repair. Nature *511*, 353–357.

Liu, L., Fuhlbrigge, R.C., Karibian, K., Tian, T., and Kupper, T.S. (2006). Dynamic programming of CD8+ T cell trafficking after live viral immunization. Immunity *25*, 511–520.

Nauta, A.J., Kruisselbrink, A.B., Lurvink, E., Willemze, R., and Fibbe, W.E. (2006). Mesenchymal stem cells inhibit generation and function of both CD34+-derived and monocyte-derived dendritic cells. J. Immunol. *177*, 2080–2087.

Postow, M.A., Callahan, M.K., and Wolchok, J.D. (2015). Immune Checkpoint Blockade in Cancer Therapy. J. Clin. Oncol. *33*, 1974–1982.

Sackstein, R. (2005). The lymphocyte homing receptors: gatekeepers of the multistep paradigm. Curr. Opin. Hematol. *12*, 444–450.

Schatton, T., Murphy, G.F., Frank, N.Y., Yamaura, K., Waaga-Gasser, A.M., Gasser, M., Zhan, Q., Jordan, S., Duncan, L.M., Weishaupt, C., et al. (2008). Identification of cells initiating human melanomas. Nature *451*, 345–349.

Schatton, T., Schütte, U., Frank, N.Y., Zhan, Q., Hoerning, A., Robles, S.C., Zhou, J., Hodi, F.S., Spagnoli, G.C., Murphy, G.F., and Frank, M.H. (2010). Modulation of T-cell activation by malignant melanoma initiating cells. Cancer Res. *70*, 697–708.

Seneschal, J., Clark, R.A., Gehad, A., Baecher-Allan, C.M., and Kupper, T.S. (2012). Human epidermal Langerhans cells maintain immune homeostasis in skin by activating skin resident regulatory T cells. Immunity *36*, 873–884.

Uccelli, A., Moretta, L., and Pistoia, V. (2008). Mesenchymal stem cells in health and disease. Nat. Rev. Immunol. *8*, 726–736.

Wang, L., Pino-Lagos, K., de Vries, V.C., Guleria, I., Sayegh, M.H., and Noelle, R.J. (2008). Programmed death 1 ligand signaling regulates the generation of adaptive Foxp3+CD4+ regulatory T cells. Proc. Natl. Acad. Sci. USA *105*, 9331–9336.